Available online at www.sciencedirect.com

ScienceDirect

Geochimica et Cosmochimica Acta 131 (2014) 138–149

Geochimica et Cosmochimica Acta

www.elsevier.com/locate/gca

Germanium isotope fractionation during Ge adsorption on goethite and its coprecipitation with Fe oxy(hydr)oxides

Oleg S. Pokrovsky [a,b,*], Albert Galy [c], Jacques Schott [a], Gleb S. Pokrovski [a], Samia Mantoura [c]

[a] *Géoscience and Environnement Toulouse, UMR 5563 CNRS, University of Toulouse, 14 Avenue Edouard Belin, 31400 Toulouse, France*
[b] *BIO-GEO-CLIM Laboratory, Tomsk State University, Tomsk, Russia*
[c] *Department of Earth Science, University of Cambridge, UK*

Received 27 July 2013; accepted in revised form 18 January 2014; Available online 1 February 2014

Abstract

Isotopic fractionation of Ge was studied during Ge adsorption on goethite and its coprecipitation with amorphous Fe oxy(hydr)oxides. Regardless of the pH, surface concentration of adsorbed Ge or exposure time, the solution–solid enrichment factor for adsorption ($\Delta^{74/70}Ge_{solution-solid}$) was $1.7 \pm 0.1\%$. The value of the $\Delta^{74}Ge_{solution-solid}$ in Fe–Ge coprecipitates having molar ratio $0.1 < (Ge/Fe)_{solid} < 0.5$ remained constant at $2.0 \pm 0.4\%$. For $(Ge/Fe)_{solid}$ ratio < 0.1, the $\Delta^{74}Ge_{solution-solid}$ increased with the decrease of Ge concentration in the solid phase, with the value as high as $4.4 \pm 0.2\%$ at $(Ge/Fe)_{solid} < 0.001$, corresponding to the majority of natural settings. These results can be interpreted based on available structural data for adsorbed and coprecipitated Ge. It follows that $Ge(OH)_4^\circ$ adsorption occurring as bidentate binuclear complexes at the goethite surface is characterised by an enrichment factor of ~1.7%, likely related to the distortion of the GeO_4 tetrahedron and the formation of Ge–O–Fe bonds at the goethite surface as compared to aqueous solution. In contrast, coprecipitation yields more distorted edge-sharing GeO_4 tetrahedra and, in the case of the most diluted samples, part of the Ge is found in coordination 6, replacing Fe(III) in octahedral positions. This produces a greater enrichment of the solid phase in lighter isotopes, mostly due to the increase in Ge–O bond distances and coordination number compared to aqueous solution, which is in line with the basic principles of isotope fractionation. Discharge of hydrothermal fluids, leading to massive $Fe(OH)_3$ precipitation in the vicinity of the springs should, therefore, represent an isotopically-heavy source of dissolved Ge to the ocean. Similarly, groundwater discharge and $Fe(OH)_3$ precipitation at the Earth's surface, Fe oxy(hydr)oxide formation in soils and riverine organo-ferric colloids coagulation, leading to iron hydroxide precipitation in estuaries, should produce an isotopically heavy Ge aqueous flux to the ocean compared to bedrock sources and particulate fluxes.

1. INTRODUCTION

Because their outer electron structures are identical, germanium and silicon are known to exhibit similar geochemical behaviours. As such, Ge has been widely used to trace both the continental and oceanic Si cycles (Froelich and Andreae, 1981; Froelich et al., 1985, 1992; Mortlock et al., 1993; Mortlock and Froelich, 1987; Filippelli et al., 2000; Derry et al., 2005, 2006). In this regard, Ge isotopes may provide useful geochemical tracers for the study of oceanic systems as well as continental weathering environments (Galy et al., 2003; Rouxel et al., 2006; Siebert et al., 2006; Qi et al., 2011; Escoube et al., 2012). Despite significant research efforts in deciphering Ge behaviour in

* Corresponding author at: Géoscience and Environnement Toulouse, UMR 5563 CNRS, University of Toulouse, 14 Avenue Edouard Belin, 31400 Toulouse, France. Tel.: +33 561332625; fax: +33 561332560.
E-mail address: oleg@get.obs-mip.fr (O.S. Pokrovsky).

http://dx.doi.org/10.1016/j.gca.2014.01.023
0016-7037/

natural systems such as hydrothermal systems (Mortlock et al., 1993; Evans and Derry, 2002; Wheat and McManus, 2008), iron-rich oceanic margin sediments (Kolodny and Halicz, 1988; King et al., 2000; Hammond et al., 2000; McManus et al., 2003), soils (Kurtz et al., 2002; Opfergelt et al., 2010; Cornelis et al., 2010), rivers (Murname and Stallard, 1990; Froelich et al., 1992; Derry et al., 2006) and biogenic minerals (Shemesh et al., 1989; Rouxel et al., 2006), the exact physical–chemical mechanisms controlling Ge at the Earth's surface remain poorly characterized. One of the main results of previous studies of Ge isotope fractionation is that Ge is tightly linked to the Fe redox cycle and Fe mineral formation in contemporary and past Earth surface environments. As a result, the use of Ge/Si as a paleoceanographic tool remains uncertain as Ge may be removed from the oceans in iron-rich sediments independent of Si (King et al., 2000). Among major natural processes governing the fractionation of Ge and its isotopes, adsorption and coprecipitation onto/with Fe oxy(hydr)oxides are extremely important for the oceanic cycle of Ge as are the non-opaline Ge sink in marine sediments (Hammond et al., 2000; King et al., 2000; McManus et al., 2003), continental weathering and colloidal transport in natural waters. At pH representative of surface weathering conditions, Ge was shown to be preferentially sorbed to Fe-oxyhydroxide surfaces by a factor of 7 relative to Si (Anders et al., 2003). On the other hand, a study of Ge behaviour in soils along a climate gradient on Hawaii demonstrated that Ge sequestration is independent of Fe redox behaviour and the precipitation of Fe-oxyhydroxides is not a major factor contributing to Ge/Si fractionation during weathering compared to Ge partitioning into secondary clay minerals (Scribner et al., 2006). A recent mass balance of dissolved Si and Ge in the ocean showed that elementary fluxes are poorly constrained, but that the non-opaline Ge sink (likely to be adsorption and coprecipitation onto/with Fe oxy(hydr)oxides) could represent between 24% and 55% of the burial flux (Mantoura et al., submitted for publication). Therefore, experimental calibration of Ge isotope fractionation linked to its interaction with iron oxides/hydroxides will clearly provide further constraints on the Ge marine and continental budget and thus constitutes the first objective of this study.

The sign and magnitude of the isotope fractionation of an element involved in a chemical reaction depend on the nature of the reaction (kinetic or equilibrium) and on the structures of the species and their associated energetic levels in the investigated reactants and products (Schauble, 2004). Structural characterization of Ge adsorbed at the goethite surface and coprecipitated with Fe oxy(hydr)oxide has been achieved using X-ray Absorption Spectroscopy (Pokrovsky et al., 2006). The present study extends this knowledge to Ge isotope fractionation during the adsorption and coprecipitation process. This should (1) allow identification and quantification of the physico-chemical factors controlling Ge isotopic variations in natural systems in the presence of Fe hydrous oxides, and (2) provide the first experimental constraints on Ge isotopic fractionation in the oxic aquatic environments of the Earth's surface.

2. MATERIALS AND METHODS

2.1. Adsorption and coprecipitation

Goethite powder, synthesized following a procedure described by Cornell and Schwertmann (1996), had a specific surface area of 23.2 m^2/g (see Pokrovsky et al., 2006 for its detailed properties). All solutions were prepared from ultrapure $NaNO_3$, HNO_3, NaOH and MilliQ water. Germanium stock solution was prepared by dissolving germanium dioxide (Fluka puriss. for electronic purposes, 99.99%) in deionized MilliQ water. Batch adsorption experiments were performed in 1 mM $NaNO_3$ background electrolyte solution using acid-cleaned 30 mL polypropylene (PP) vials, which were agitated for 2 days on a RotaMag® mixer at 25 ± 0.5 °C. Four concentrations of goethite powder were used: 1.8, 3.3, 6.6 and 17 g/L, and initial Ge concentration in solution ranged from 344 to 384 μM. At the end of experiments, the solution pH was measured, the suspension was centrifuged for 15 min at 2500*g*, filtered through pre-cleaned 0.22 μm acetate cellulose sterile disposable filters, and the supernatant was acidified by bi-distilled HNO_3 prior to analyses. During filtration, the first 5–10 mL of the filtrate were discarded to allow filter material rinsing and porespace saturation. In order to evaluate possible artifacts linked to Ge chemical and isotopic fractionation during sample filtration, standard Ge solution of neutral pH and concentration similar to that in experimental samples, was filtered and analysed for total Ge concentration and Ge isotope ratio (sample "Blank Ge no ads"). This filtration procedure did not modify dissolved Ge concentration more than 2%, and the isotopic ratio of filtered standard solution was similar, within ± 0.1‰, to δ^{74}Ge of the unfiltered initial solution.

The kinetics of Ge adsorption was studied in a batch stirred reactor through which N_2 was continuously bubbled. N_2 bubbling was intended to avoid oxygen interferences with goethite surface, but mostly to remove the dissolved CO_2 that is capable of forming adsorbed carbonate and bicarbonate complexes, and thus compete with Ge for goethite binding sites. In these experiments, 1 mM $NaNO_3$ solution with 6.6 g/L of goethite powder was used, and pH was kept constant at 8.50 ± 0.05. Aliquots of goethite suspension were removed and immediately filtered for subsequent chemical and isotopic analyses.

Germanium coprecipitation with iron oxy(hydr)oxide was performed at 25 °C in 30 mL PP vials via slow oxidation of the 0.8 mM Fe(II) sulfate solutions in 0.1 M $NaNO_3$ by atmospheric oxygen. Values of pH varied from 4.6 to 10.4, and the initial Ge concentration ($[Ge]_o$) varied from 16 to 930 μM. Amorphous iron oxy(hydr)oxide was formed during the first 0.5–1.0 h of reaction and allowed to age for 24 h. This yielded Ge concentration in the solid phase corresponding to molar ratio Ge/Fe of 0.02–0.5. Note that aging of precipitates for 1–14 days at 25 °C in contact with solutions open to the atmosphere did not produce any significant change in Ge and Fe aqueous concentrations. Another method of Ge coprecipitation with iron hydroxide consisted of neutralizing a 900 μM Fe(III) acidic solution (made from $Fe(NO_3)_3$ in 0.1 M $NaNO_3$ at pH 2) by the

addition of 2% NH_4OH until pH reached ~6.5–7.5. All precipitates were separated from solution by centrifugation for 10 min at 4000 rpm, rinsed in MilliQ water, and dried for 72 h at 60 °C.

2.2. Chemical analyses

Solution pH was measured using a combination glass electrode (Mettler Toledo) calibrated on the activity scale with NIST pH buffers (pH = 4.006, 6.865, and 9.180 at 25 °C). The precision of pH measurements was ±0.002 units (0.1 mV). Total germanium ($[Ge]_{tot}$) concentration was measured by flame atomic absorption using a Perkin Elmer 5100 PC spectrometer in the concentration range of 30–800 μmol L^{-1} with an uncertainty of 2%. For Ge analyses in the concentration range of 1.4–140 μmol L^{-1}, a colorimetric method with molybdenum blue was used (uncertainty of 2%). Finally, at very low concentrations ($[Ge] < 7$ μmol L^{-1}), dissolved germanium was determined by ICP-MS (Elan 6000, Perkin Elmer) using ^{70}Ge and ^{74}Ge isotopes. Indium and rhenium were used as internal standards, and the international geostandard SLRS-4 (Riverine Water Reference Material for Trace Metals certified by the National Research Council of Canada) was used to check the validity and reproducibility of the analyses. This freshwater standard has low concentrations of major ions and was similar in ionic strength to the majority of our experimental solutions. The uncertainty of ICP-MS analyses was 10% at $[Ge] < 0.014$ μmol $L^{-1}$and 5% at $[Ge] \geqslant 0.014$ μmol L^{-1}. The three methods of Ge analysis employed in this study agreed within 5%. The Ge blank in our experiments, a typical aqueous solution prepared as in the experiments but without Ge added, was between 30 and 60 pg. Total dissolved iron (Fe(II) + Fe(III)) was measured by flame atomic absorption spectroscopy (AAS) using a Perkin Elmer 5100 PC spectrometer in the concentration range of 3.6–90 μmol L^{-1} with an uncertainty of 2% and a detection limit of 0.9 μmol L^{-1}. Fe concentration in the solid was measured by AAS after dry sample dissolution in concentrated HNO_3, with an uncertainty of 5%. This uncertainty corresponded to the mean 2σ of five repeat measurements of an in-house standard solution.

2.3. Ge isotopic measurements

Ge-isotope ratios were measured using a Nu Instruments MC-ICPMS and a sample-standard bracketing protocol (Galy et al., 2003). Briefly, ^{70}Ge, ^{72}Ge, ^{73}Ge and ^{74}Ge were collected in Faradays Low 3, Axial, High 2 and High 4 respectively within the overall array. Standard and sample isotope values were measured 4 and 3 times, respectively for 200 s each. Each 200 s measurement consisted of 5 s integration of the electronic background by deflecting the ion beam at the electrostatic analyser followed by 100 s acquisition of the signal, repeated twice. This protocol allows the calculation of 6 brackets, and each value corresponds to their average. Isotopic compositions are expressed as a permil deviation from the isotopic composition of the standard solution as follows:

$$\delta^{x}Ge(‰) = \left\{ \left({}^{x}Ge/{}^{70}Ge\right)_{sample} / \left({}^{x}Ge/{}^{70}Ge\right)_{Standard} - 1 \right\} \times 1000$$

where $x = 72$, 73 or 74.

Because of the lack of an international isotopic standard of germanium, a commercial germanium standard solution (with a germanium concentration of 1000 μg g^{-1}) in 2% KOH (Aldrich, USA) was used as our in-house isotopic standard. Its long-term reproducibility was close to 0.1% for $\delta^{74}Ge$.

Filtered aqueous solutions of adsorption experiments (Fig. 1) were measured in dry plasma mode, where samples and standards were introduced into the plasma torch through an Aridus desolvating nebuliser (Galy et al., 2003). This device minimises the introduction of H_2O, CO_2, O_2 and N_2 into the plasma. Elution on a column of AG 50 W-X8 cationic resin with 0.5 M HNO_3 allowed the separation of germanium from the alkali matrix. The chemistry yield was found to be ⩾90% as quantified by comparing the ICP-MS measured total dissolved Ge concentration in solution and converting in total mass of Ge before and after the ion exchange column separation procedure. The external repeatability (replicate analyses on different days) of in-house isotopic standard (commercial germanium standard solution) measured over 8 months was observed to be 0.12%, 0.16% and 0.07% for $\delta^{74}Ge$ $\delta^{73}Ge$ and $\delta^{72}Ge$,

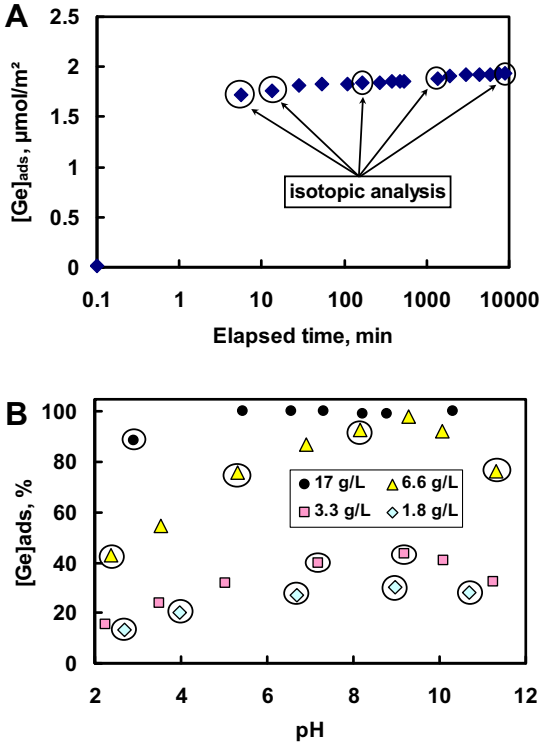

Fig. 1. Concentration of adsorbed germanium in contact with goethite as a function of time, obtained from aqueous solution analysis (A) and pH dependence of Ge adsorption on goethite at various solid/solution ratios (B). In both cases, the final solution of a separate experiment was analysed. The error bars are within the symbol size. Aqueous solution samples used for isotopic analysis are circled.

respectively. The standard-sample-standard bracketing technique used to examine repeatability of measurements yielded a stability of the uncorrected $^{74}Ge/^{70}Ge$ ratio during extended runs of up to 12 h of close to 0.12% per hour.

As a part of the evolution of the Ge isotopic method, selected coprecipitation experiments (Fig. 2) were measured using a continuous flow hydride generation system coupled to the MC-ICPMS (Rouxel et al., 2006, Mantoura et al., submitted for publication). The reducing agent (a solution of 0.26 N of $NaBH_4$ stabilized in 0.0125 N of NaOH) and the sample were introduced to the hydride generation (HG) system by a peristaltic pump. The separation of the gas from the liquid has been achieved with the use of a modified Scott-type spray chamber cooled at 4 °C and a PTFE filter between the spray chamber and the ICP-MS torch. Stability of hydride formation was improved by the use of a mixing coil (20 cm), consistent pumping of the liquid waste to the drain, and a second Ar inlet placed between the spray chamber and the ICP-MS torch. The decontamination of the inlet was achieved by the use of a solution of diluted HNO_3 (2%) for 5 min. Given that all the solutions introduced into MC ICP MS were prepared at similar Ge concentration and that the relative isotopic difference between different samples was within few%, the cross-contamination of the succeeding sample was <0.5% of the previous Ge intensity measured and thus did not require any specific correction. The external repeatability of replicate analyses of in-house isotopic standard on different days was observed to be 0.14%, 0.12% and 0.09% for $\delta^{74}Ge$ $\delta^{73}Ge$ and $\delta^{72}Ge$, respectively. While this method is marginally less precise than the dry plasma mode, it allows direct measurement without the removal of alkali matrix by chemical purification and also has a greater sensitivity. The consistency between the two methods was verified using aqueous solutions produced after Ge adsorption on goethite labelled Ge2 and Ge4 in Galy et al. (2003) work (Table 2 of Galy et al., 2003). The typical difference between two methods ranged between 0.05% and 0.08% on $\delta^{74}Ge$ value which did not exceed the external error (Rouxel et al., 2006; Mantoura et al., submitted for publication). The typical internal uncertainty on the $\delta^{74}Ge$ value in measured liquid and solid samples ranged between 0.05% and 0.10%. 5 samples of coprecipitation experiments exhibited higher internal uncertainty, between 0.1% and 0.3%, which could be linked to low Ge concentration and the presence of relatively high Fe in solution, yielding some instability of the signal during the sample bracketing procedure. One sample (4–2, Table 2) exhibited large analytical uncertainty (±0.77% on $\delta^{74}Ge$) and as such was not used for data analyses. This sample had the lowest Ge concentration (Table 2) and as a result, the lowest stability of the signal. Values of $\delta^{74}Ge$, $\delta^{73}Ge$ and $\delta^{72}Ge$ for samples measured in this study plot along the expected mass fractionation line with an average deviation ($2\sigma_{mean}$) of $-0.013 \pm 0.006\%$ and $0.001 \pm 0.007\%$ from the slopes of 0.5137 and 0.6754 for $\delta^{74}Ge$ versus $\delta^{72}Ge$ and $\delta^{73}Ge$ versus $\delta^{72}Ge$, respectively.

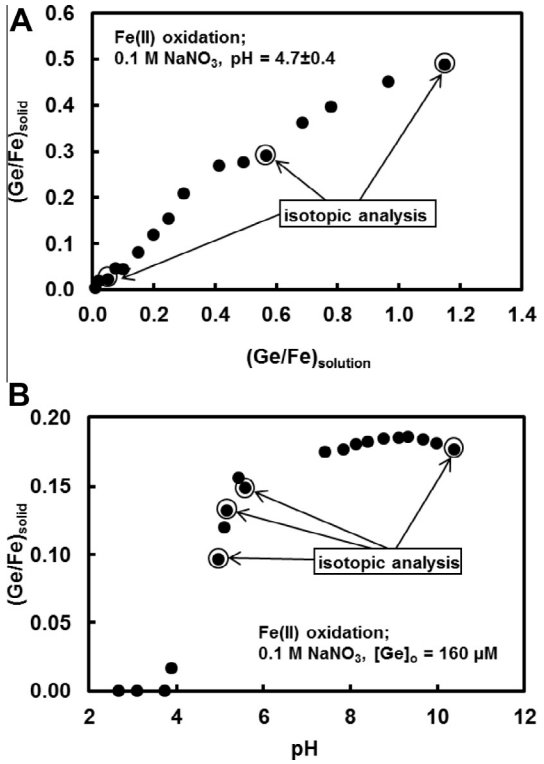

Fig. 2. Germanium coprecipitation with Fe oxy(hydr)oxide formed by oxidation of Fe(II) salt at constant pH and variable initial Ge concentration shown as Ge/Fe molar ratio in the solid phase versus Ge/Fe ratio in the aqueous phase at the beginning of reaction (A, series 4 of Table 2) and versus aqueous solution pH at constant initial Ge concentration (B, series 5 of Table 2). Exposure time is 24 h.

For all isotopic measurements of this study, filtered aqueous solutions were used because of their much higher sensitivity to the minor changes in isotopic composition compared to the bulk solid. This contrasts with some other studies of stable isotope fractionation during adsorption, when both liquid and solid phases were processed and measured (ca. Goldberg et al., 2009; Beard et al., 2010). Assuming that the loss of Ge in our batch adsorption and coprecipitation experiments is solely accounted for by the goethite surface, or coprecipitation with Fe oxy(hydr)oxide, the Ge isotope ratio of the solid phase ($\delta^{74}Ge_{solid}$) can be calculated from the mass balance equation using the isotopic ratio in the aqueous phase ($\delta^{74}Ge_{solution}$), the fraction of Ge removed from the solution (F, % of the initial amount), and the isotope ratio of the initial solution used for experiments ($\delta^{74}Ge_{initial}$):

$$\delta^{74}Ge_{solid} = \left(100 \times \delta^{74}Ge_{initial} - (100 - F) \times \delta^{74}Ge_{solution}\right)/F \quad (1)$$

A similar approach to calculating the isotopic composition of the solid phase, based on the mass balance equation and the isotopic composition of the measured aqueous phase, was used for Mo (Barling and Anbar, 2004), Cu and Zn (Balistrieri et al., 2008) and Si adsorption on mineral surfaces (Delstanche et al., 2009). We carefully verified the absence of experimental artifacts in the Ge mass balance calculation during sample handling and filtration. In particular, in isotopic fractionation experiments, full recovery of filtered solution during the preparation procedure is crucial (Barling and Anbar, 2004). Filtration

of supernatant in adsorption type experiments did not affect the fractionation coefficients because filtration of the initial Ge stock solution did not change $\delta^{74}Ge$ within the uncertainty (±0.1%) as verified by (i) Multi Collector ICP MS measurements on this filtered sample subjected to the column purification procedure, and (ii) a 100 ± 1% recovery of $[Ge]_{aq}$ in filtered standard solutions at pH 5–6 as measured by AAS and ICP MS.

The difference in the isotopic composition of Ge in solution and Ge adsorbed and/or incorporated in the solid phase is reported with the usual notation:

$$\Delta^{74}Ge_{solution-solid} = \delta^{74}Ge_{solution} - \delta^{74}Ge_{solid} \quad (2)$$

The estimated uncertainties on calculated $\Delta^{74}Ge_{solution-solid}$ values stem from (1) the uncertainty in the proportion of adsorbed Ge (F parameter in Eq. (2), (2) the analytical uncertainty on the initial isotopic composition of the Ge solution used in adsorption or coprecipitation experiments, and (3) the analytical uncertainty on Ge isotopic ratio in each individual experiment. As a result, the overall uncertainty on $\Delta^{74}Ge_{solution-solid}$ is a factor of 1.5–2 higher than that on $\delta^{74}Ge_{solution}$, and it strongly increases at low fractions of adsorbed or coprecipitated Ge. Since, for most experiments, only the aqueous phase was analysed, we evaluated the associated errors via measuring total Ge retained in the solid phase. After full acid digestion of the solid, we found a recovery of Ge between 90% and 95%. Assuming the "worst" scenario, 90% recovery, we calculated the error produced in the final ($\Delta^{74}Ge_{solution-solid}$) calculation for each data point from Eqs. (2) and (1). This overall uncertainty given in Table 2 was estimated numerically, individually for each experiment based on respective uncertainties on F and $\delta^{74}Ge_{solution}$ values.

3. RESULTS

An overview of the conducted experiments and the main experimental conditions is given in Table 1. Concentrations of adsorbed germanium in contact with goethite as a function of time and pH are presented in Fig 1 A and B, respectively. For coprecipitation experiments, the Ge/Fe ratio in the solid as a function of this ratio in solution and solution pH is shown in Fig. 2A and B, respectively.

3.1. Adsorption

Adsorption of aqueous Ge onto goethite surface is fast (1–10 h), fully reversible and pH-dependent (Pokrovsky et al., 2006). For the pH dependence, the bell-shaped form of the sorption envelope, with a sorption maximum for a solution pH close to the pK of H_4GeO_4 first dissociation constant (~9), is typical of weak acids (i.e., H_3BO_3, H_4SiO_4).

The evolution of aqueous Ge isotopic composition ($\Delta^{74}Ge_{solution}$) as a function of% adsorbed Ge is shown in Fig. 3A. It can be seen that the $\Delta^{74}Ge_{solution-solid}$ remained constant (Fig. 3B) within the uncertainty of measurements and equals 1.69 ± 0.08% (2 sd, $n = 17$), where error reflects propagated uncertainties from the multiple source of error. This demonstrates that isotopic equilibrium is reached between the solution and the solid surface and corroborates the reversible nature of the adsorption as witnessed by recovery of the initial Ge solution concentration by reverting the pH (Pokrovsky et al., 2006). Neither the effect of Ge surface concentration (from 0.8 to 2.6 μmol/m^2 goethite, Fig. 4A) nor pH (from 2.5 to 11.3, Fig. 4B) on the isotopic fractionation factor of Ge during adsorption on goethite could be resolved beyond the experimental uncertainty. It is also important to note that all four different concentrations of goethite examined in this study yielded identical $\Delta^{74}Ge_{solution-solid}$ values (1.58 ± 0.07, 1.65 ± 0.10, 1.75 ± 0.03, and 1.75 ± 0.18% for 17, 6.6, 3.3, and 1.8 g/L of goethite, respectively) at $2\sigma_{mean}$ level. Finally, the effect of equilibration time (from 0.1 to 150 h) on the isotopic fractionation between the aqueous solution and goethite surface was found to be negligible at our experimental conditions (Table 2, experiments 5–1 to 5–17).

3.2. Coprecipitation

The rate of Ge coprecipitation with Fe hydroxides is similar to the rate of Ge adsorption: stable concentration of incorporated Ge is achieved after ~1.5 h of exposure in a wide range of solution pH (Pokrovsky et al., 2006). Both the initial $(Ge/Fe)_{solution}$ ratio and the final pH exert a major control on Ge incorporation into the solid (Fig. 2).

The solid phase formed during iron hydroxide precipitation via Fe^{2+} oxidation or Fe^{3+} hydrolysis and stored 24 h in mother solution is an iron hydroxide containing 12 ± 3 wt% of water regardless of the presence of Ge (Pokrovsky et al., 2006). The (Ge/Fe) ratio in the precipitated solids exerted the major control on the crystallinity of the solid phase: amorphous Fe hydroxide is always formed at $(Ge/Fe)_{solid} > 0.05$. For $0.02 \leqslant (Ge/Fe)_{solid} \leqslant 0.05$, well crystallized lepidocrocite was identified in our samples, that

Table 1
Synthesis of all conducted experimental and the range of experimental conditions.

Experiment no.	Type of interaction	Duration	Goethite (g/L) or [Fe]aq (mg/L)	pH range	Ge range, μM
1 Ads to 7 Ads	Adsorption	48 h	3.3–17 g/L	2.9–11.3	24–207
IV-1 to IV-5	Adsorption	48 h	1.8 g/L	2.7–10.7	250–332
5–1 to 5–17	Adsorption	0.1–150 h	6.6 g/L	8.5	39–73
4–2 to 4–16	Coprecipitation during Fe(II) oxidation	26 h	13–45 mg/L	5.0–5.3	16–930
5–3 to 5–18	Coprecipitation during Fe(II) oxidation	24 h	0.01–160 mg/L	5.0–10.4	0.1–160
C-16	Coprecipit., Fe(III) Hydrolysis	26	10.5 mg/L	6.7	52–275
C-17	Coprecipit., Fe(II) oxidation	26	93 mg/L	4.6	200–275

Table 2
Experimental data measured in this study. The 2σ standard deviation is based on 3–4 measurements of the same sample.

Adsorption	% Ge_{ads}	$[Ge]_{init}$ μmol L^{-1}	$[Ge]_{final}$ μmol L^{-1}	pH	Goethite g/L	Ge_{ads} μmol/m^2	Time, h	$\delta^{74}Ge$ ‰	2σ	$\delta^{73}Ge$ ‰	2σ	$\delta^{72}Ge$ ‰	2	Nb	$\delta^{74}Ge_{solid}$ ‰	$\Delta^{74}Ge$ solution–solid
Blank Ge no ads	0	344						−0.01	0.09	−0.02	0.08	−0.01	0.06	9		
1 Ads	88.7	344	39	2.9	17	0.8	48	1.40	0.02	1.01	0.05	0.68	0.03	2	−0.19	1.58 ± 0.07
2 Ads	75.2	344	85	5.5	6.6	1.7	48	1.09	0.02	0.80	0.03	0.55	0.04	10	−0.37	1.46 ± 0.10
3 Ads	92.9	344	24	8.16	6.6	2.1	48	1.56	0.10	1.17	0.06	0.78	0.07	3	−0.13	1.69 ± 0.09
4 Ads	76.3	344	82	11.31	6.6	1.7	48	1.06	0.32	0.78	0.21	0.53	0.19	3	−0.34	1.39 ± 0.35
5 Ads	40.0	344	207	2.5	6.6	0.9	48	0.72	0.16	0.54	0.09	0.35	0.07	6	−1.10	1.82 ± 0.40
6 Ads	40.0	344	207	7.18	3.3	1.8	48	0.71	0.04	0.52	0.05	0.34	0.03	3	−1.08	1.79 ± 0.20
7 Ads	43.7	344	194	9.20	3.3	2.0	48	0.74	0.01	0.55	0.05	0.38	0.02	3	−0.97	1.72 ± 0.25
IV-0 Initial soln.	0	344						−0.10	0.07	−0.09	0.05	−0.06	0.04	6		
IV1	13.0	381	332	2.68	1.8	1.2	48	0.09	0.05	0.07	0.05	0.03	0.04	3	−1.43	1.52 ± 0.40
IV-2	20.4	384	306	3.98	1.8	1.9	48	0.22	0.05	0.14	0.04	0.10	0.03	3	−1.38	1.60 ± 0.37
IV-3	27.3	370	269	6.70	1.8	2.4	48	0.40	0.07	0.30	0.09	0.19	0.03	3	−1.46	1.86 ± 0.25
IV-4	30.0	357	250	8.97	1.8	2.6	48	0.51	0.10	0.34	0.06	0.25	0.06	4	−1.53	2.04 ± 0.30
IV-5	28.2	376	270	10.7	1.8	2.5	48	0.38	0.10	0.29	0.11	0.19	0.07	5	−1.35	1.73 ± 0.35
Exp no. 5, Kinetics in 0.001M $NaNO_3$																
5–1	78.8	343	73	8.5	6.6	1.8	0.1	1.34	0.11	1.00	0.06	0.65	0.04	2	−0.37	1.71 ± 0.13
5–2	81.0	343	65	8.5	6.6	1.8	0.2	1.47	0.09	1.09	0.10	0.72	0.05	2	−0.36	1.83 ± 0.11
5–6	84.3	343	54	8.5	6.6	1.9	2.8	1.48	0.11	1.07	0.20	0.73	0.08	3	−0.28	1.76 ± 0.12
5–11	85.7	343	49	8.5	6.6	1.9	23	1.33	0.09	0.97	0.14	0.63	0.04	3	−0.22	1.55 ± 0.11
5–17	88.6	343	39	8.5	6.6	2.0	150	1.47	0.05	1.16	0.04	0.74	0.03	2	−0.19	1.67 ± 0.07
Co-precipitation			$[Ge]_{init}$ μmol L^{-1}	$[Ge]_{final}$ μmol L^{-1}	pH	(Ge/Fe) mol	Fe, mg/L	$\delta^{74}Ge$‰	2σ	$\delta^{73}Ge$‰	2σ	$\delta^{72}Ge$ ‰	2σ	Nb	$\delta^{74}Ge_{solid}$‰	$\Delta^{74}Ge$ solution–solid
Blank 4–5	Initial solution						45	0.05	0.01	−0.02	0.00	0.04	0.07	2		
4–2[b]	$Fe(II)SO_4$ oxidation		16.1		4.99	0.030	14.5	1.62	0.77	1.27	0.58	0.85	0.36	2	0.05	1.57 ± 0.80
4–12	At different Ge_0		456	322	5.14	0.292	19.2	0.77	0.32	0.55	0.19	0.37	0.16	4	−1.67	2.44 ± 0.60
4–16	$[Fe]_{init} = 45$ mg/L		927	649	5.27	0.493	13.2	0.54	0.07	0.41	0.07	0.27	0.05	3	−1.08	1.62 ± 0.26
5–3	$Fe(II)SO_4$ oxidation		160	119	4.97	0.097	21.2	0.76	0.25	0.55	0.14	0.39	0.11	3	−1.98	2.74 ± 0.75
5–7			160	87	5.17	0.134	14.4	1.17	0.30	0.88	0.22	0.59	0.13	3	−1.29	2.46 ± 0.66
5–9	$[Fe]_{init} = 45$ mg/L		160	47	5.59	0.141	2.52	1.56	0.10	1.19	0.14	0.80	0.09	3	−0.57	2.14 ± 0.14
5–18			160	17	10.38	0.178	0.01	1.28	0.37	0.96	0.29	0.65	0.17	3	−0.10	1.38 ± 0.41
C-16[a]	Fe(III) hydrolysis		275	52	6.68	0.276	10.5	1.74	0.18	1.32	0.14	0.91	0.10	3	−0.34	2.08 ± 0.52
C-17[b]	Fe(II) oxidation		275	196	4.59	0.047	93	1.11	0.06	0.85	0.04	0.59	0.04	2	−2.53	3.64 ± 0.20

[a] Fe(III) hydrolysis (1 mM Fe^{3+}).
[b] Fe(II) oxidation, $[Fe^{2+}]_{init} = 188$ mg/L.

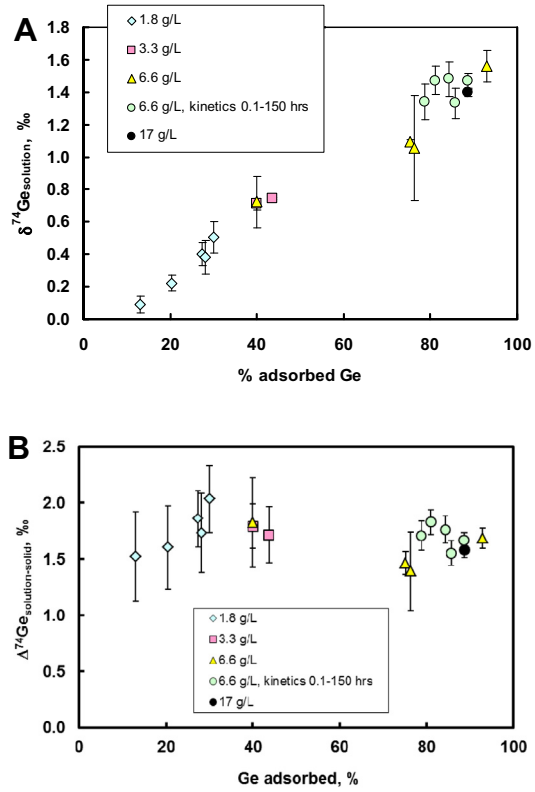

Fig. 3. Plot of the aqueous δ^{74}Ge value (A) and isotopic shift (B) between aqueous solution and solid phase for Ge adsorption at the surface of goethite. Diamonds, squares, triangles, open and closed circles denote experiments with different goethite concentration of 1.8, 3.3, 6.6 (reversible adsorption and kinetics) and 17 g/L, respectively.

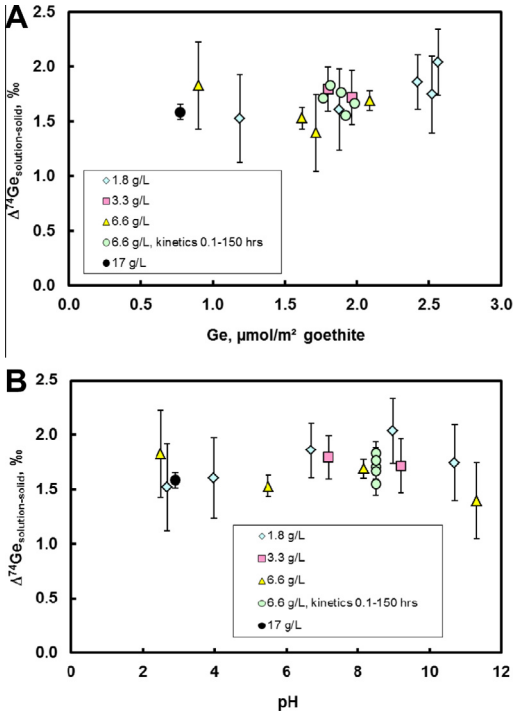

Fig. 4. Isotopic shift of ^{74}Ge between solution and solid measured in adsorption experiments as a function of Ge surface concentration (A) and solution pH (B).

recrystallized into goethite upon aging in mother solution at ambient temperature (Pokrovsky et al., 2006).

The value of δ^{74}Ge in the fluid phase is positively correlated ($r^2 = 0.68$) with the amount of Ge coprecipitated with iron hydroxide (Fig. 5A). The $\Delta^{74}Ge_{solution-solid}$ is not correlated to the pH of the solution (Fig. 5B) or the $(Ge/Fe)_{solid}$ ratio (Fig. 6) at 95% confidence ($r^2 < 0.5$). At the same time, it is not excluded that the most and the least fractionated samples are retrieved from the lowest and the highest pH experiments, respectively (Fig. 5B). There are two trends of $\Delta^{74}Ge_{solution-solid}$ dependence on $(Ge/Fe)_{solid}$: a constant value at $(Ge/Fe)_{solid} > 0.2$ and a linear ($r^2 = 0.97$ at $p = 0.95$) trend at $(Ge/Fe)_{solid} < 0.2$ with an intercept at +4.43%. A distinct difference in $\Delta^{74}Ge_{solution-solid}$ is observed for the most diluted samples (3.19 ± 0.48% for Ge/Fe < 0.1, calculated as the average of two low concentration samples C-17 and 5–3, Table 2), compared to the most concentrated ones (2.02 ± 0.43% for $0.1 < Ge/Fe < 0.5$). The precipitation mode, either Fe(II) oxidation or Fe(III) hydrolysis, does not have any significant effect on the resulting $\Delta^{74}Ge_{solution-solid}$ value (Figs. 5 and 6). The effect of the crystallinity of the formed precipitate, lepidocrocite versus amorphous Fe hydroxide, on Ge isotopic fractionation between aqueous solution and resulting precipitates could not be resolved beyond the uncertainty of our measurements. Overall, the $\Delta^{74}Ge_{solution-solid}$ characteristic of coprecipitation processes was 0.3–2% higher than that associated with Ge adsorption on goethite.

4. DISCUSSION

4.1. Factors responsible for Ge isotope fractionation

Several structural/chemical factors may be responsible for Ge isotope fractionation during adsorption and coprecipitation processes in aqueous solution: (i) germanic acid protonation in solution and at the mineral surface; (ii) goethite surface coverage, which may control Ge binding to weak sites of high abundance versus low abundance strong sites; (iii) Ge binding mode, i.e., bidentate versus monodentate and binuclear versus mononuclear; (iv) Ge–O bond distances, the identity of the second neighbor, and the degree of distortion of the 1st coordination sphere; and finally, (v) Ge coordination in solution and in the solid phase, i.e., tetrahedral versus octahedral. All or some of these factors determine the equilibrium isotope fractionation between Ge at the goethite surface or in the Fe oxy(hydroxide) lattice and aqueous solution and control the fractionation kinetics during irreversible coprecipitation phenomena.

The effect of the first factor, germanic acid protonation/deprotonation at the goethite surface on Ge isotopic fractionation can be tested by comparing the $\Delta^{74}Ge_{solution-solid}$ among experiments of different equilibrium pH (Fig. 4B). According to the surface complexation model for Ge speciation at the goethite surface (Pokrovsky et al., 2006), $\geqslant$90% of adsorbed Ge is present as neutral > FeO–$Ge(OH)_3^\circ$ species at pH < 5–6 whereas in alkaline solutions,

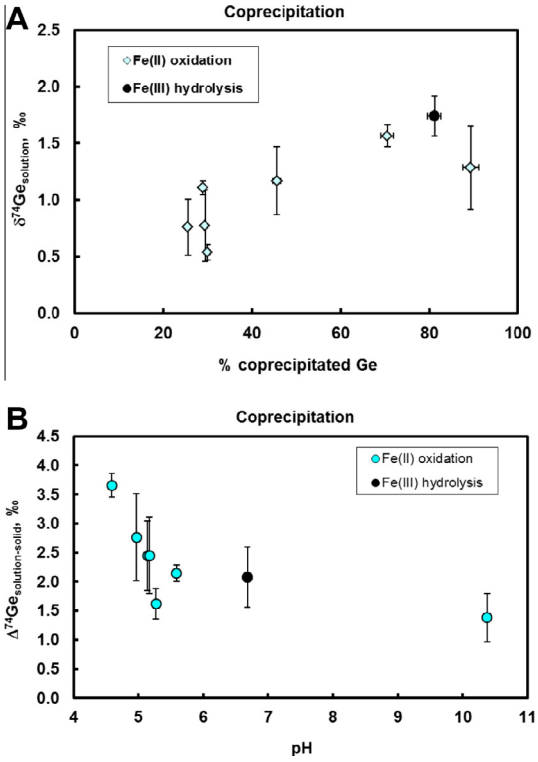

Fig. 5. Plots of the isotopic composition of the fluid phase as a function of Ge fraction coprecipitated in the solid (A) and the shift between solution and solid phase versus solution pH (B). The horizontal error bars are within the symbol size (from 1% to 2% in A and 0.01 pH units in B) unless shown.

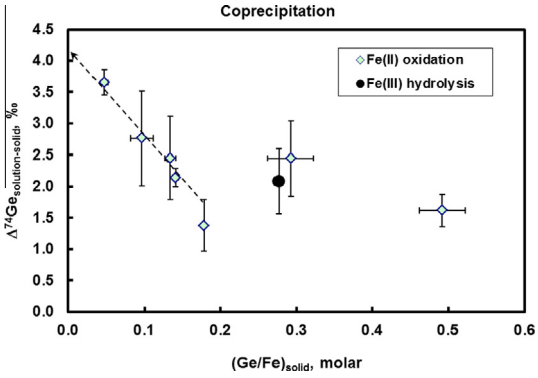

Fig. 6. Effect of the Ge/Fe ratio in the solid phase on overall ^{74}Ge isotopic shift between aqueous solution and precipitated Fe oxy(hydr)oxide. The vertical error bars were numerically calculated by error propagation whereas the horizontal error bars mostly reflect the analytical uncertainty. Arrowed dashed line shows a linear extrapolation, without taking into account sample 4–2. The left-hand end of this dashed line corresponds to the low concentrations of natural samples, which yields $\delta^{74}Ge_{solution-solid} = 4.43 \pm 0.20‰$ at Ge/Fe < 0.001.

at pH of 10, half of the adsorbed Ge is represented by deprotonated > FeO–Ge(OH)$_2^-$ species. Because the solution pH exhibits a minor effect on $\delta^{74}Ge_{solution-solid}$ (Fig. 5B), it can be concluded that the degree of protonation of Ge(O,OH)$_4$ tetrahedra at the goethite surface does not impact Ge isotopic fractionation between aqueous solution and the goethite surface.

The role of the 2nd factor is also likely to be small as follows from the lack of a statistically significant relationship between $\Delta^{74}Ge_{solution-solid}$ and the Ge surface concentration (30–100% of goethite surface site occupied, Fig. 4A). This strongly suggests that the degree of goethite surface coverage by sorbed Ge that can encounter either weak or strong binding sites does not affect the $\Delta^{74}Ge_{solution-solid}$ value for adsorption.

The 3rd and 4th factors can be tested using available data on the structure of the complexes formed on goethite surface by germanic acid and other similar neutral molecules and oxyanions (Pokrovsky et al., 2006 and references therein). These data suggest that Ge is adsorbed in the form of binuclear complexes, and 1:1 stoichiometry between Ge(aq) and >FeOH surface sites is always maintained as two Fe centers interact with two Ge tetrahedra. This model is supported by XANES and EXAFS results demonstrating (1) the tetrahedral Ge environment (within ±10% of XAS uncertainty) for all adsorption samples, and (2) the distance of 3.3 ± 0.1 Å between Ge and 0.5–1 Fe atom as the second neighbor corresponding to double-corner bi-dentate (C_2-type) complexes between the Ge-tetrahedra and two adjacent Fe-octahedra sharing a common edge at the goethite surface (Fig. 7A). At the same time, given the average nature of an EXAFS signal, Ge atomic environment may be multiple, particularly at the high surface coverage here, with different complexes simultaneously present at the FeOOH surface as shown in Fig. 7B.

The enrichment of lighter isotopes at the surface during the adsorption reaction can be explained by the change of next-nearest environment of the adsorbed atom. Indeed, even at similar Ge–O distances between aqueous and adsorbed Ge tetrahedra, the appearance of the second neighbour, such as Fe in adsorbed samples, leads to a decrease in the symmetry and an increase in the disorder compared to the aqueous Ge tetrahedron. Second, the formation of bidendendate tetrahedral binuclear complexes (C_2-type, Fig. 7), and tetrahedral complexes sharing their edges with Fe octahedra (E-type, Fig. 7), is likely to increase their distortion and the disorder among Ge positions due to higher number of possible geometries. This should be accompanied by a decrease of the stability of Ge-ligand bonds in the first coordination sphere and, in accord with the principles of quantum mechanics, by an enrichment of the solid phase in lighter isotopes. Similar mechanisms of solid phase enrichment in lighter isotopes compared to the aqueous solution could operate for other oxyanions and neutral molecules such as MoO_4^{2-} (Barling and Anbar, 2004) and Si(OH)$_4$ (Delstanche et al., 2009). For example, Mo adsorbed on birnessite is known to form a polynuclear structure with distorted octahedral coordination compared to tetrahedrally coordinated MoO_4^{2-} in aqueous solution, which produces 2.7% in $\delta^{98/95}$Mo enrichment in lighter isotopes at the surface (Wasylenki et al., 2011).

The effect of the last factor, the tetrahedral (Ge^{IV}) versus octahedral (Ge^{VI}) environment, on Ge isotopic fractionation during its interaction with Fe oxy(hydr)oxide could

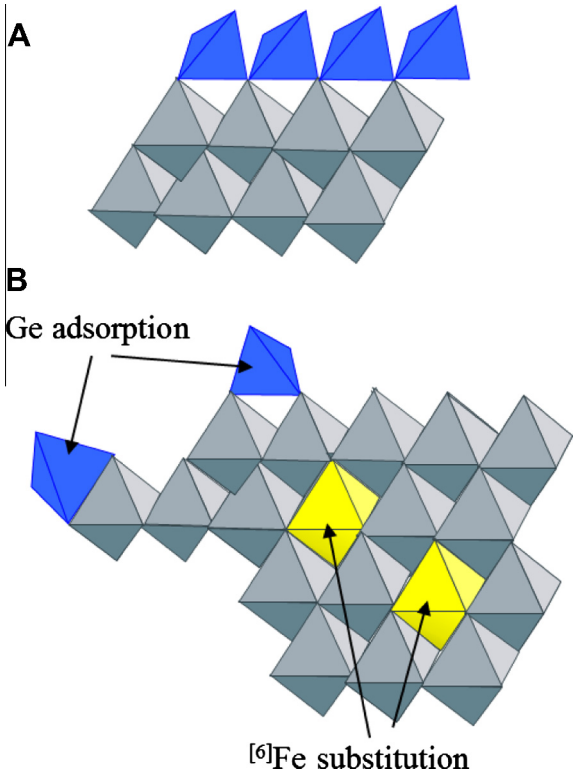

Fig. 7. Schematic structures of the atomic environment of Ge(IV) adsorbed onto or co-precipitated with Fe(III) oxy-hydroxides. (A): Bidentate binuclear adsorbed complexes that maintain 1:1 stoichiometry between Fe surface centers and $Ge(OH)_4$ in case of adsorption experiments, notably at high surface coverages, producing average fractionation $\Delta^{74}Ge_{solution-solid}$ of $1.69 \pm 0.08‰$. (B): Bidentate mononuclear (E-type) and bidentate binuclear (C_2-type) complexes of tetrahedral Ge and octahedral $^{[6]}Ge$ substitution for Fe octahedral in the bulk of Fe oxy(hydr)oxides in case of Ge coprecipitation with Fe oxy(hydr)oxide, producing possible fractionation $\Delta^{74}Ge_{solution-solid}$ of $4.43 \pm 0.20‰$. Light-grey octahedra denote the $Fe(O/OH)_6$ coordination sphere with the metal in the centre; blue tetrahedra and yellow octahedra stand for Ge(IV) four- and six-coordinated with O/OH, respectively. (For interpretation of the references to colour in this figure legend, the reader is referred to the web version of this article.)

only be probed on coprecipitated samples that exhibited a partial Ge^{VI} environment (Pokrovsky et al., 2006). The significant increase of $\Delta^{74}Ge_{solution-solid}$ for samples C-17 and 5–3 (Table 2), which correspond the lowest Ge concentration in the solid phase, may be linked to the change of Ge local structure in these diluted samples. Indeed, according to XAS results, samples with Ge/Fe < 0.1 exhibit a splitting of the first atomic shell, with Ge in both tetrahedral ($R = 1.77 \pm 0.02$ Å, $N = 3.0$–3.5) and octahedral ($R = 1.92 \pm 0.03$ Å, $N = 0.5$–1.3) coordination with oxygen, in contrast to the samples having a Ge/Fe > 0.1 (Pokrovsky et al., 2006). It is therefore likely that $\varepsilon_{solution-solid}$ will tend to be greater for GeO_6, which exhibits larger Ge–O distances and thus weaker Ge–O bonds compared to GeO_4 both in the aqueous solution and the solid (i.e., see Criss, 1999; Schauble et al., 2004). If we assume that $\varepsilon_{solution-solid}$ for Ge^{VI} ($\varepsilon_{solution-solid}{}^{VI}$) is greater than $\varepsilon_{solution-solid}$ for Ge^{IV} ($\varepsilon_{solution-solid}{}^{IV}$) but remained constant through the coprecipitation and that the experiments are at isotopic equilibrium, then it can easily be demonstrated that the observed $\delta^{74}Ge_{solution-solid}$ is linearly correlated with the proportion of Ge^{VI} in Ge. Given that the fraction of octahedral Ge in samples studied in this work is (1) rather low, and (2) only observed in solid with Ge/Fe < 0.1 suggesting a very low Ge^{VI}/Fe, the Ge/Fe ratio of the solid is a good approximation of the proportion of Ge^{VI} in the solid. As a result, the extrapolation of $\delta^{74}Ge_{solution-solid}$ to $(Ge/Fe)_{solid} = 0$ will give a good approximation of $\varepsilon_{solution-solid}{}^{VI}$ (Fig. 6). This extrapolation was performed for the most diluted samples with $(Ge/Fe)_{solid} < 0.2$ and yielded $\delta^{74}Ge_{solution-solid} = 4.4 \pm 0.2‰$ (2σ at $p = 0.95$) in infinitely diluted sample ($r^2 = 0.97$ without sample No. 4–2). This value should be regarded as tentative given (i) the low number of experimental data points used to carry out the correlation and (ii) the high experimental uncertainties on individual data points used to calculate the extrapolated value.

Overall, the obtained experimental results confirm recent first-principles density functional theory calculation of Ge adsorbed onto Fe oxy(hydr)oxide surfaces (Li and Liu, 2010). These authors demonstrated that Ge isotopes can be distinctly fractionated by such adsorption processes, to about 1.7%.

It is interesting to note that the $\varepsilon_{solution-solid}$ for Si, which forms bidentate binuclear complexes at the goethite surface similar to germanium complexes (Vempati and Loeppert, 1989; Pokrovsky et al., 2006) is ~2–3 times lower ($\Delta^{29}Si_{solution-solid} = 0.54$ and 0.81‰; Delstanche et al., 2009) than the corresponding $\varepsilon_{solution-solid}$ for Ge, whereas the differences in the reciprocal of the square root of isotope masses for $^{74/70}Ge$ and $^{29/28}Si$ (Criss, 1999 and reference therein) are almost the same. The lighter isotopic composition of adsorbed Ge compared to Si may be explained by the more distorted structure of the Ge complexes present at the goethite surface. Indeed, the formation of bidendate binuclear (C_2-type) Si and Ge complexes yields a distance between two oxygen atoms at the goethite surface equals to 2.6 Å (Szytula et al., 1968; Manceau, 1995) and Si–O and Ge–O bond lengths equal to 1.65 Å (Newton and Gibbs, 1980) and 1.76 Å (Pokrovsky et al., 2006), respectively. This induces a decrease of the O–(Si,Ge)–O angle from 109.5° in the aqueous species to 104° and 95° in the adsorbed Si and Ge tetrahedral, respectively. At the same time, the Mo oxyanion is also known to form complexes similar to Ge (Bibak and Borggaard, 1994), and exhibits comparable $\varepsilon_{solid-solution}$ (~2‰, Barling et al., 2001; Siebert et al., 2003; Barling and Anbar, 2004; Goldberg et al., 2009; Wasylenki et al., 2011) despite a difference in the reduced mass (smaller by 68%).

An important and poorly studied aspect of Ge geochemistry in natural ferric oxy(hydr)oxides is the presence in the latter of Si and/or Al as impurities (e.g., Blanch et al., 2008; Silva et al., 2010). These trace components may certainly compete with Ge for specific binding sites at the goethite surface and thus change the overall fractionation factor between the mineral and the aqueous solution, as is known for other oxyanions (Silva et al., 2010). However, we do not

anticipate a significant effect of these impurities as our adsorption data do not suggest the existence of strong (low abundant) versus weak (highly abundant) binding sites for Ge isotopes (Figs. 3B and 4A). As such, any competition between Ge and these components in nature is rather unlikely.

4.2. Geochemical applications

Results obtained in the present study allow straightforward evaluation of the degree of Ge isotope fractionation in natural settings where the formation of Fe oxy(hydr)oxide occurs. Two basic cases can be considered, when Ge-bearing waters interact with Fe-rich sediments or soils and when co-precipitation of Ge occurs during the oxidation of Fe(II) and the massive formation of Fe(III)oxyhydroxide. The majority of natural settings can be approximated by the room temperature used in the present study to quantify Ge isotope fractionation between aqueous solution and Fe oxyhydroxides. Since diffusion (transport) processes do not control Ge adsorption and coprecipitation, as follows from fast reaction kinetics (Pokrovsky et al., 2006), we do not expect a significant effect of temperature on isotope fractionation. However, similar to other oxyanions (Wasylenki et al., 2008), some decrease of the isotopic fractionation with temperature increase may occur.

Note that the first natural case, the infiltration of Ge-bearing fluids through Fe(III)-bearing soils or sediments, should prompt an enrichment of the fluid phase in heavier isotopes, proportional to the amount of Ge, up to the $\varepsilon_{solution-solid}$ value of $1.69 \pm 0.08\%$. Such a Ge isotope fractionation can be expected in groundwaters in contact with Fe(III)-rich clays or sandstones or, in the case of surface water interaction, with saprolite soils. Thus, tropical rivers draining highly weathered magmatic rocks could be enriched in δ^{74}Ge by 1–1.5% relative to the unaltered bedrocks. In the case of Fe oxy(hydr)oxide precipitation in marine or freshwater sediments within pore fluids or bottom water layers, the enrichment of the liquid phase in heavier isotopes should be much higher given the possibility of repeated cycles and Rayleigh distillation in a closed pore space, as is known for other isotopic couples; e.g., δ^{57}Fe values can vary up to 7% in sediment porewaters of subterranean estuaries (Rouxel et al., 2008).

Ge coprecipitation with Fe oxyhydroxide includes the following settings (i) hydrothermal spring discharges in the ocean or on the continent, within the volcanic provenances, where massive Fe oxy(hydr)oxide formation occurs mediated by Fe(II) oxidation; (ii) secondary Fe hydroxide formation in soils; (iii) acid mine drainage and Fe(III) precipitation along the flow path; (iv) Fe(II) oxidation during groundwater discharge at the earth surface; and (v) Fe(III) coagulation in the estuarine zone. The first example is found at the top of the plumes above hydrothermal vents near oceanic ridges (i.e., Mortlock et al., 1993) where significant amounts of Ge can be retained by iron hydroxide, thus enriching the output fluid and oceanic water in heavier isotopes (Mantoura et al., submitted for publication). Both acid mine drainage and groundwater Fe(II) oxidation lead to preferential coprecipitation of lighter Ge isotopes with newly formed amorphous Fe oxy(hydr)oxides, thus enriching the small rivers, seepage zones, and streams in heavier isotopes. Indeed, the emergence of reduced underground waters is often followed by the precipitation of iron oxy(hydr)oxides in the vicinity of springs. In such settings, a decrease of the Ge/Si ratio in the fluid induced by the preferential scavenging of Ge has already been invoked (Anders et al., 2003). Moreover, Ge-rich goethite and hematite from the weathering zone of the copper-arsenic sulfide Apex Mine (Utah, USA) were reported to contain octahedrally coordinated Ge in samples with $(Ge/Fe)_{solid} \sim 0.01$ (Bernstein and Waychunas, 1987). Our experimental results strongly suggest that in such a setting, secondary minerals will have δ^{74}Ge ca. 3–4% lower than the δ^{74}Ge of the fluid and, presumably, the source rock.

The process of oxidation of groundwater Fe(II) is also known to occur at the riparian or the hyporheic zones of organic-rich streams in the boreal zone, where formation of Fe(III)-colloids stabilized by dissolved organic matter of allochthonous origin occurs (Pokrovsky and Schott, 2002). These colloids (1 kDa–0.22 μm in size), being represented by Fe(III) hydroxide globules with incorporated trace elements, are likely to have light Ge isotopic signatures relative to the truly dissolved low molecular weight (<1 kDa) Fe-poor fraction. Massive coagulation of these isotopically light colloids, and thus preservation of the isotopically-heavy low molecular weight fraction in the mixing zone between freshwater and seawater (Pokrovsky et al., 2012) should, again, lead to an enrichment of the ocean in heavier isotopes relative to source rocks. As such, all major processes of Fe oxyhydroxide formation at the earth surface should lead to enrichment of the fluid, and notably its most labile LMW fraction, in heavier isotopes, which will subsequently be delivered to the ocean by small surface streams as drivers. Note that secondary Fe oxy(hydr)oxide formation in soils should also take up the lighter Ge isotopes from pore fluids, receiving Ge either from the source minerals or the plant litter and phytolith. As a result, surface waters draining Fe(III)-rich soils such as laterites should be significantly enriched in heavier isotopes relative to the source rock.

Given that the majority of natural settings with Ge–Fe coprecipitation reactions imply very low Ge/Fe ratios in the fluid and, consequently, in the solid phase, it is tempting to assume very high fractionations, up to 4% $\varepsilon_{solution-solid}$, in some specific settings of Fe–rich, Ge–poor waters. Such high $\varepsilon_{solution-solid}$ could have an enhanced effect on the Ge isotopic composition of the fluid by Rayleigh distillation. Taken together, it is conceivable that Ge interaction with Fe- oxy(hydr)oxides would raise the δ^{74}Ge of the ocean waters by $2.0 \pm 1.0\%$ compared to continental crust, which spans the range of $\Delta^{74}Ge_{solution-solid}$ encountered in the present work during adsorption and coprecipitation. This is a very conservative estimate because it implies the absence of Ge fractionation during host silicate rock dissolution. In addition, it suggests the lack of Ge fractionation linked to biogenic Si production and its equivalent dissolution in the water column.

5. CONCLUSIONS

Our systematic study of Ge interaction with Fe oxy (hydr)oxides in aqueous solutions revealed the first-order features of isotope fractionation linked to major physical–chemical parameters of the media and structural changes of adsorbed and incorporated Ge. The enrichment of the goethite in lighter Ge isotopes relative to aqueous solution is a factor of two higher than that for Si. Ge coprecipitation that produces octahedral ($^{[VI]}$Ge) environment, could have a $\varepsilon_{solution-solid}^{VI}$ more than twice the $\varepsilon_{solution-solid}^{IV}$. In the sequence of studied samples, "adsorption → concentrated co-precipitates → diluted co-precipitates", our previous XAS measurements confirm the increase of the distances between Ge and O and the increase of the proportion of corner-sharing $^{[6]}$Ge octahedral positions via substitution of Ge for Fe in the bulk amorphous Fe oxy(hydr)oxide. This suggests bond weakening between Ge and surrounding ligands leading to the progressive enrichment of adsorption/coprecipitation products by lighter isotopes. Given the range of isotopic fractionation between aqueous solution and Fe oxy(hydr)oxide measured in our experiments, the most likely difference in the δ^{74}Ge between the hydrosphere and the upper continental crust ranges between 1‰ and 3‰.

ACKNOWLEDGEMENTS

We are grateful to Associate Editor Derek Vance and three anonymous reviewers for their insightful and constructive comments. This work was supported by the grant of the Russian ministry of Science and Education No 14.B25.31.0001 (BIO-GEO-CLIM). Merlin Méheut (GET, Toulouse) is warmly thanked for insightful discussions on the stable isotope fractionation theory.

REFERENCES

Anders A. M., Sletten R. S., Derry L. A. and Hallet B. (2003) Germanium/silicon ratios in the Copper River Basin, Alaska: weathering and partitioning in periglacial versus glacial environments. *J. Geophys. Res.* **108**(F1), 6005.

Balistrieri L. S., Borrok D. M., Wanty R. B. and Ridley W. I. (2008) Fractionation of Cu and Zn isotopes during adsorption onto amorphous Fe(III) oxyhydroxide: experimental mixing of acid rock drainage and ambient river water. *Geochim. Cosmochim. Acta* **72**, 311–328.

Barling J. and Anbar A. D. (2004) Molybdenum isotope fractionation during adsorption by manganese oxides. *Earth Planet. Sci. Lett.* **217**, 315–329.

Barling J., Arnold G. L. and Anbar A. D. (2001) Natural mass-dependent variations in the isotopic composition of molybdenum. *Earth Planet. Sci. Lett.* **193**, 447–457.

Beard B. L., Handler R. M., Scherer M. M., Wu L., Czaja A. D., Heimann A. and Johnson C. M. (2010) Iron isotope fractionation between aqueous ferrous iron and goethite. *Earth Planet. Sci. Lett.* **295**, 241–250.

Bernstein L. R. and Waychunas G. A. (1987) Germanium crystal chemistry in hematite and goethite from the Apex Mine, Utah, and some new data on germanium in aqueous solution and in stottite. *Geochim. Cosmochim. Acta* **51**, 623–630.

Bibak A. and Borggaard O. K. (1994) Molybdenum adsorption by aluminum and iron oxides and humic acid. *Soil Sci.* **158**, 323–328.

Blanch A. J., Quinton J. S., Lenehan C. E. and Pring A. (2008) The crystal chemistry of Al-bearing goethites: an infrared spectroscopic study. *Mineral. Mag.* **72**(5), 1043–1056.

Cornell R. M. and Schwertmann U. (1996) *The Iron: Structure, Properties, Reactions Occurrences and Uses*. VCH, Weinheim.

Cornelis J.-T., Delvaux B., Cardinal D., André L., Ranger J. and Opfergelt S. (2010) Tracing mechanisms controlling the release of dissolved silicon in forest soil solutions using Si isotopes and Ge/Si ratios. *Geochim. Cosmochim. Acta* **74**, 3913–3924.

Criss R. E. (1999) *Principles of Stable Isotope Distribution*. Oxford University Press, Oxford.

Delstanche S., Opfergelt S., Cardinal D., Elsass F., André L. and Delvaux B. (2009) Silicon isotopic fractionation during adsorption of aqueous monosilicic acid onto iron oxide. *Geochim. Cosmochim. Acta* **73**, 923–934.

Derry L. A., Kurtz A. C., Ziegler K. and Chadwick O. A. (2005) Biological control of terrestrial silica cycling and export fluxes to watersheds. *Nature* **433**, 728–731.

Derry L. A., Pett-Ridge J. C., Kurtz A. C. and Troester J. W. (2006) Ge/Si and 87Sr/86Sr traces of weathering reactions and hydrological pathways in a tropical granitoid system. *J. Geochem. Explor.* **88**, 271–274.

Escoube R., Rouxel O. J., Luais B., Ponzevera E. and Donard O. F. X. (2012) An intercomparison study of the germanium isotope composition of geological reference materials. *Geostand. Geoanal. Res.* **36**(2), 149–159.

Evans M. J. and Derry L. A. (2002) Quartz control of high germanium/silicon ratios in geothermal waters. *Geology* **30**, 1019–1022.

Filippelli G. M., Carnahan J. W., Derry L. A. and Kurtz A. (2000) Terrestrial paleorecords of Ge/Si cycling derived from lake diatoms. *Chem. Geol.* **168**, 9–26.

Froelich P. N. and Andreae M. O. (1981) The marine geochemistry of germanium-Ekasilicon. *Science* **213**, 205–207.

Froelich P. N., Hambrick G. A., Andreae M. O., Mortlock R. A. and Edmond J. M. (1985) The geochemistry of inorganic germanium in natural waters. *J. Geophys. Res.* **90**, 1133–1141.

Froelich P. N., Blanc V., Mortlock R. A., Chilrud S. N., Dunstan W., Udomkit A. and Peng T. H. (1992) River fluxes of dissolved silica to the ocean were higher during glacials: Ge/Si in diatoms, rivers, and oceans. *Paleoceanography* **7**, 739–767.

Galy A., Pomies C., Day J. A., Pokrovsky O. S. and Schott J. (2003) High precision measurement of germanium isotope ratio variations by multiple collector-inductively coupled plasma spectrometry. *J. Anal. At. Spectrom.* **18**, 115–119.

Goldberg T., Archer C., Vance D. and Poulton S. W. (2009) Mo isotope fractionation during adsorption to Fe (oxyhydr)oxides. *Geochim. Cosmochim. Acta* **73**, 6502–6516.

Hammond D. E., McManus J., Berelson W. M., Meredith C., Klinkhammer G. P. and Coale K. H. (2000) Diagenetic fractionation of Ge and Si in reducing sediments: the missing Ge sink and a possible mechanism to cause glacial/interglacial variations in oceanic Ge/Si. *Geochim. Cosmochim. Acta* **64**, 2453–2465.

King S. L., Froelich P. N. and Jahnke R. A. (2000) Early diagenesis of germanium in sediments of the Antartic South Atlantic: in search of the missing Ge sink. *Geochim. Cosmochim. Acta* **64**, 1375–1390.

Kolodny Y. and Halicz L. (1988) The geochemistry of germanium in deep-sea cherts. *Geochim. Cosmochim. Acta* **52**, 2333–2336.

Kurtz A. C., Derry L. A. and Chadwick O. A. (2002) Germanium–silicon fractionation in the weathering environment. *Geochim. Cosmochim. Acta* **66**, 1525–1537.

Li X. F. and Liu Y. (2010) First-principles study of Ge isotope fractionation during adsorption onto Fe(III)-oxyhydroxide surfaces. *Chem. Geol.* **278**(1–2), 15–22.

McManus J., Hammond D. E., Cummins K., Klinkhammer G. K. and Berelson W. M. (2003) Diagenetic Ge–Si fractionation in continental margin environments: further evidence for a non-opal Ge sink. *Geochim. Cosmochim. Acta* **67**, 4545–4557.

Manceau A. (1995) The mechanism of anion adsorption on iron oxides: evidence for the bonding of arsenate tetrahedra on free Fe(O,OH)6 edges. *Geochim. Cosmochim. Acta* **59**, 3647–3653.

Mantoura S., De La Rocha C. L., Galy A., Latimer J. C. and Shemesh A. (submitted for publication) Germanium isotopes and trace elements in diatom silica: glacial–interglacial records and constraints on the oceanic germanium isotope cycle. *Geochim. Cosmochim. Acta*.

Mortlock R. A. and Froelich P. N. (1987) Continental weathering of germanium: Ge/Si in the global river discharge. *Geochim. Cosmochim. Acta* **51**, 2075–2082.

Mortlock R. A., Froelich P. N., Feely R. A., Massoth G. J., Butterfield D. A. and Lupton J. E. (1993) Silica and germanium in Pacific Ocean hydrothermal vents and plumes. *Earth Planet. Sci. Lett.* **119**, 365–378.

Murname R. J. and Stallard R. F. (1990) Germanium and silicon in rivers of the Orinoco drainage basin. *Nature* **344**, 749–752.

Newton M. D. and Gibbs G. V. (1980) Ab initio calculated geometries and charge distributions for H_4SiO_4 and $H_2Si_2O_7$ compared with experimental values for silicates and siloxanes. *Phys. Chem. Miner.* **6**, 221–246.

Opfergelt S., Cardinal D., André L., Delvigne C., Bremont L. and Delvaux B. (2010) Variations of δ^{30}Si and Ge/Si with weathering and biogenic input in tropical basaltic ash soils under monoculture. *Geochim. Cosmochim. Acta* **74**, 225–240.

Pokrovsky O. S. and Schott J. (2002) Iron colloids/organic matter associated transport of major and trace elements in small boreal rivers and their estuaries (NW Russia). *Chem. Geol.* **190**, 141–179.

Pokrovsky O. S., Pokrovski G. S., Schott J. and Galy A. (2006) Experimental study of germanium adsorption on goethite and germanium coprecipitation with iron hydroxide: X-ray absorption fine structure and macroscopic characterization. *Geochim. Cosmochim. Acta* **70**, 3325–3341.

Pokrovsky O. S., Viers J., Dupré B., Chabaux F., Gaillardet J., Audry S., Prokushkin A. S., Shirokova L. S., Kirpotin S. N., Lapitsky S. A. and Shevchenko V. P. (2012) Biogeochemistry of carbon, major and trace elements in watersheds of Northern Eurasia drained to the Arctic Ocean: the change of fluxes, sources and mechanisms under the climate warming prospective. *C.R. Geosci.* **344**, 663–677.

Qi H.-W., Rouxel O. and Hu R.-Z., et al. (2011) Germanium isotopic systematics in Ge-rich coal from the Lincang Ge deposit, Yunnan Southwestern China. *Chem. Geol.* **286**(3–4), 252–265.

Rouxel O., Galy A. and Elderfield H. (2006) Germanium isotopic variations in igneous rocks and marine sediments. *Geochim. Cosmochim. Acta* **70**, 3387–3400.

Rouxel O., Sholkovitz E., Charette M. and Edwards K. J. (2008) Iron isotope fractionation in subterranean estuaries. *Geochim. Cosmochim. Acta* **72**(14), 3413–3430.

Schauble E. A. (2004) Applying stable isotope fractionation theory to new systems. *Rev. Mineral. Geochem.* **55**, 65–111.

Schauble E. A., Rossman G. R. and Taylor, Jr., H. P. (2004) Theoretical estimates of equilibrium chromium–isotope fractionations. *Chem. Geol.* **205**, 99–114.

Scribner A. M., Kurtz A. C. and Chadwick O. A. (2006) Germanium sequestration by soil: targeting the roles of secondary clays and Fe-oxyhydroxides. *Earth Planet. Sci. Lett.* **243**, 760–770.

Shemesh A., Mortlock R. A. and Froelich P. N. (1989) Late Cenozoic Ge/Si record of marine biogenic opal: implications for variations in riverine fluxes to the ocean. *Paleoceanography* **4**, 221–234.

Siebert C., Nägler T. F., von Blanlenburg F. and Kramers J. D. (2003) Molybdenum isotope records as a potential new proxy for paleoceanography. *Earth Planet. Sci. Lett.* **211**, 159–171.

Siebert C., Ross A. and McManus J. (2006) Germanium isotope measurements of high-temperature geothermal fluids using double-spike hydride generation MC-ICP-MS. *Geochim. Cosmochim. Acta* **70**, 3986–3995.

Silva J., Mello J. W. V., Gasparon M., Abrahao W. A. P., Ciminelli V. S. T. and Jong T. (2010) The role of Al-goethites on arsenate mobility. *Water Res.* **44**, 5684–5692.

Szytula A., Burewicz A., Dimitrijewic Z., Krasnicki S., Rzany H., Todorovic J., Wanic A. and Wolski W. (1968) Neutron diffraction studies of α-FeOOH. *Phys. Status Solidi* **26**, 429–434.

Vempati R. K. and Loeppert R. H. (1989) Influence of structural and adsorbed Si on the transformation of synthetic ferrihydrite. *Clays Clay Miner.* **37**, 273–279.

Wasylenki L. E., Rolfe B. A., Weeks C. L., Spiro T. G. and Anbar A. D. (2008) Experimental investigation of the effects of temperature and ionic strength on Mo isotope fractionation during adsorption to manganese oxides. *Geochim. Cosmochim. Acta* **72**, 5997–6005.

Wasylenki L. E., Weeks C. L., Bargar J. R., Spiro T. G., Hein J. R. and Anbar A. D. (2011) The molecular mechanism of Mo isotope fractionation during adsorption to birnessite. *Geochim. Cosmochim. Acta* **75**, 5019–5031.

Wheat C. G. and McManus J. (2008) Germanium in mid-ocean ridge flank hydrothermal fluids. *Geochem. Geophys. Geosyst.* **9**(3). http://dx.doi.org/10.1029/2007GC001892.

Associate editor: Derek Vance